UNUSUAL FIBROUS SODIAN TAINIOLITE EPITACTIC ON PHLOGOPITE FROM MARBLE XENOLITHS OF MONT SAINT-HILAIRE, QUEBEC, CANADA

Thomas ARMBRUSTER[§]

Laboratorium für chemische und mineralogische Kristallographie,Universität Bern, Freiestr. 3, CH–3012 Bern, Switzerland

R. Peter RICHARDS

National Center for Water Quality Research, Heidelberg College, Tiffin, Ohio 44883, USA

Edwin GNOS, Thomas PETTKE and Marco HERWEGH

Institut für Geologie, Universität Bern, Balzerstr. 1, CH–3012 Bern, Switzerland

Abstract

Samples of marble xenoliths, thermally metamorphosed by the igneous rocks of Mont Saint-Hilaire, Quebec, contain idiomorphic plates of phlogopite. These plates were later overgrown and to some extent topotactically replaced by sodian tainiolite, tapering in fragile fibers extending parallel to [100]. The fibers only protrude parallel to [100] of the phlogopite host. Unit-cell parameters of phlogopite and tainiolite, both $1M$ polytypes (space group $C2/m$), are so similar that the phases in the phlogopite–tainiolite intergrowth could not be distinguished by single-crystal X-ray methods. Phlogopite of composition $K_{1.01}(Mg_{1.96}Fe_{0.66}Li_{0.20}Mn_{0.03}Ti_{0.03}Al_{0.04})_{\Sigma 2.92}(Si_{3.28}Al_{0.72})_{\Sigma 4}O_{10}[(OH)_{1.14}F_{0.86}]_{\Sigma 2}$ has the highest Si/Al value of natural samples of phlogopite known to us. The epitactic fibers of tainiolite, of composition $K_{1.01}(Mg_{2.00}Fe_{0.01}Li_{0.59}Na_{0.38})_{\Sigma 2.98}(Si_{3.99}Al_{0.01})_{\Sigma 4}O_{10}[F_{1.79}Cl_{0.01}(OH)_{0.20}]_{\Sigma 2}$, represent to our knowledge the first example of an extended solid-solution, established by combined electron-microprobe and laser-ablation mass-spectrometry analyses, between tainiolite, $K(LiMg_2)Si_4O_{10}F_2$, and the recently described mineral shirokshinite, $K(NaMg_2)Si_4O_{10}F_2$. The latest mineral formed in the observed paragenesis is the zeolite mesolite, accompanied by an unidentified aluminosilicate with Ca/K $\approx$ 1.

Keywords: phlogopite, tainiolite, shirokshinite, mica, fibers, epitactic growth, Mont Saint-Hilaire, Quebec.

Sommaire

Des enclaves de marbre, thermiquement métamorphisées par les venues ignées du mont Saint- Hilaire, Quebec, contiennent des cristaux idiomorphes de phlogopite. Ces cristaux ont ensuite subi une surcroissance et, jusqu'à un certain point, un remplacement topotactique par la tainiolite sodique, s'effilant en fibres fragiles allongées, seulement parallèles à [100]. Les paramètres réticulaires de la phlogopite et de la tainiolite, les deux correspondant au polytype $1M$ (groupe d'espace $C2/m$), se ressemblent si étroitement que les phases dans l'intercroissance de phlogopite et de tainiolite n'ont pas pu être distinguées par diffraction X sur monocristaux. La phlogopite, de composition $K_{1.01}(Mg_{1.96}Fe_{0.66}Li_{0.20}Mn_{0.03}Ti_{0.03}Al_{0.04})_{\Sigma 2.92}(Si_{3.28}Al_{0.72})_{\Sigma 4}O_{10}[(OH)_{1.14}F_{0.86}]_{\Sigma 2}$, possède la valeur Si/Al la plus élevée des échantillons naturels de phlogopite que nous connaissons. Les fibres épitactiques de tainiolite, de composition $K_{1.01}(Mg_{2.00}Fe_{0.01}Li_{0.59}Na_{0.38})_{\Sigma 2.98}(Si_{3.99}Al_{0.01})_{\Sigma 4}O_{10}[F_{1.79}Cl_{0.01}(OH)_{0.20}]_{\Sigma 2}$, représenteraient le premier exemple d'une solution solide étendue, établie par une combinaison d'analyses avec une microsonde électronique et par plasma à couplage inductif avec spectrométrie de masse, entre tainiolite, $K(LiMg_2)Si_4O_{10}F_2$, et la shirokshinite, $K(NaMg_2)Si_4O_{10}F_2$, espèce minérale établie récemment. Le dernier minéral à s'être formé dans les enclaves est la mésolite, du groupe des zéolites; il est accompagné par un aluminosilicate méconnu ayant un rapport Ca/K environ égal à 1.

(Traduit par la Rédaction)

Most-clés: phlogopite, tainiolite, shirokshinite, mica, fibres, croissance épitactique, Mont Saint-Hilaire, Québec.

[§] *E-mail address*: thomas.armbruster@krist.unibe.ch

Introduction

Epitactic relations among crystals (*i.e.*, structural coherency relations), or more generally, epitactic growth, are of special interest not only in material science (production of composite materials), but also in nature, where a host crystal provides the substrate for the crystallization of a guest mineral without the necessity to overcome the energy-barrier associated with nucleation. This process strongly influences crystallization kinetics, leads to puzzling habits, and may favor metastable crystallization.

In this paper, we report on the epitactic growth of tainiolite, a trioctahedral mica of ideal composition $K(LiMg_2)Si_4O_{10}F_2$, on phlogopite, another trioctahedral mica of simplified end-member composition $KMg_3(AlSi_3)O_{10}(OH)_2$. The sample originates from marble xenoliths of the alkaline igneous rocks at Mont Saint-Hilaire, Quebec, Canada. At first glance, one may expect rather isotropic overgrowth of one sheet silicate on the other. However, in the example investigated, epitactic tainiolite crystallizes with a fibrous habit, and all fibers exhibit a uniform orientation relative to the phlogopite host.

Geological Setting and Sample Description

Mont Saint-Hilaire (MSH) is located about 40 km east of Montreal, in southwestern Quebec. It is one of the Monteregian Hills, a series of alkaline igneous stocks of Cretaceous age located along an east–southeast trend that extends eastward 120 km from Oka, Quebec, west of Montreal. These stocks have been interpreted as a sequence of stationary vents for mantle-derived materials and heat (Currie *et al.* 1986) associated with the St. Lawrence rift system (Currie 1970). The geology of the Monteregian Hills, and of Mont Saint-Hilaire in particular, is described in Currie (1970, 1983), Greenwood & Edgar (1984), and Currie *et al.* (1986).

The Poudrette Quarry is developed in rocks of the East Hill suite, which is a product of the last intrusive event. Among the products of this event is a pipe of nepheline and sodalite syenites, phonolites, and intrusive breccias containing many xenoliths of older igneous and sedimentary rocks, including a massive block of Ordovician sediments that was engulfed by the magma and transformed to hornfels (Van Velthuisen 1990). Well-formed crystals of a wide variety of minerals have been recovered from pockets in these rocks. The complex geochemistry and petrogenesis have produced many paragenetically complex associations involving one mineral replacing or overgrowing another, generally epitactically oriented.

The samples for this study were collected by Richards on October 24, 2004 from a pectolite zone in a marble xenolith. This xenolith was not seen in place. Consequently, we do not know the identity of the host rock. Whereas marble xenoliths at Mont Saint-Hilaire have been interpreted as clasts of Precambrian basement incorporated into the rising magmas, at least some xenoliths must be younger because they contain fossils (McDonald & Chao 2004). In 1994, Richards found a brachiopod replaced by pectolite and sodic amphibole. Although the sample was found loose in the quarry, the mineral composition is characteristic of the marble xenoliths. The specimen, now in the Canadian Museum of Nature, has been identified as a spiriferid, probably of early Silurian age (McDonald & Chao 2004). The part of the xenolith from which the samples were collected is characterized by a loose, sugary texture, and includes well-formed crystals of dolomite and pectolite to 2 cm and mm-sized crystals of albite, which in turn are coated with small crystals of quartz and locally with the epitactic association and other minerals reported here. Some of the dolomite has an epitactic overgrowth of calcite.

Experimental

Phlogopite flakes with the epitactic fibers parallel to (001) were extracted under a binocular microscope and mounted either for an X-ray single-crystal study on glass fibers or on a conducting carbon tab for subsequent study with a scanning electron microscope (SEM, Camscan CS4) and chemical identification by energy-dispersive spectroscopy (EDS, Pioneer light element detector and Voyager 4 system of analysis). The crystals were carbon-coated. The same mount was later embedded in epoxy, polished and used for quantitative chemical analyses with a JEOL 8200 electron microprobe (EMP) equipped with wavelength-dispersive spectrometers. Measurement times of 20–30 seconds on peak and background, beam conditions of 15 kV, 20 nA, and a spot 5 μm in diameter were chosen. Natural or synthetic silicate and oxide standards were used for calibration. The data were corrected using the $\phi(\rho Z)$ algorithm (Armstrong 1995). Detection limits for K, Na, Ca and Cl are 0.01 wt.%, 0.02% for Si, Ti, Cr, Al, Mg and Mn, 0.06% for Fe and 0.10% for F.

The micas embedded in epoxy (the same crystals as investigated by EMP and SEM) were analyzed for Li using laser-ablation inductively coupled plasma – mass spectrometry (LA–ICP–MS) at the Institute of Geological Sciences in Bern. The instrument consists of a pulsed 193 nm ArF Excimer laser (Lambda Physik, Germany) with an energy-homogenized Geolas Pro optical system (Microlas, Germany), coupled with an ELAN DRC–e ICP quadrupole mass spectrometer (Perkin Elmer, Canada) operated in standard mode. The laser energy used was *ca.* 6 J cm^{-1}. Operating conditions were similar to those reported in Pettke *et al.* (2004). A laser spot 30–50 μm in diameter was used for sample ablation. Five spots for tainiolite and three spots for phlogopite were sampled. Data were reduced with the Lamtrace program, using the electron-microprobe data on K_2O for tainiolite and phlogopite as internal stan-

dard. The SRM 610 glass from NIST was used as the external standard to calibrate analyte sensitivities.

The X-ray single-crystal study on two composite phlogopite–tainiolite assemblages was performed with an Enraf Nonius CAD4 diffractometer using graphite-monochromatized Mo$K\alpha$ X-radiation. In addition, reciprocal-space X-ray-diffraction images were displayed with a CCD camera of a Bruker SMART 1 K system. The goal of these experiments was to explore the epitactic relationship between the two sheet silicates by analyzing the overlay of the reciprocal lattices of host and guest crystals and to determine polytype and cell dimensions at high scattering-angles.

RESULTS

Epitactic relations are best explored by applying a combination of X-ray crystal-orientation determination and SEM imaging using the mode for back-scattered-electron (BSE) images. The BSE technique generates compositional contrast: owing to the higher density (higher average atomic number), the host crystal appears brighter than the darker epitactic guest (Figs. 1a–d). Corresponding images indicate that the host crystal (phlogopite) is overgrown or topotactically replaced by tainiolite. At a later stage of overgrowth, the tainiolite tapers to fibers: all fibers obey structural coherence relations and extend along [100] of phlogopite. In no case did we find fibers extending parallel to [110] or [$\bar{1}$10], which also are expected directions of growth owing to the pseudohexagonal symmetry of mica sheets. The blocks of tainiolite (Fig. 1d) growing on (010) of phlogopite appear particularly fragile because fiber growth is parallel to the contact plane. The blocks also tend to split because they are subperpendicular to the (001) cleavage of both minerals. Some phlogopite crystals display dissolution steps on the (001) surface (Figs. 1a–c). Such holes are filled with fibrous aggregates of tainiolite without obvious relation in orientation to the host crystal (e.g., Fig. 1b).

Results of electron-microprobe and LA–ICP–MS analyses represent averages measured on two specimens. They are summarized in Table 1, and compared with similar compositions of mica from MSH and other localities. No apparent chemical zoning was detected in phlogopite. Homogeneously and compactly overgrown tainiolite does not show chemical differences to the fine fibers of tainiolite, which formed last. The lithium content of phlogopite (0.64 wt.% Li$_2$O) is striking. We reject the hypothesis that this Li content is due to local contamination of tainiolite replacing phlogopite (e.g., Fig. 1c). In LA–ICP–MS analyses, we also monitored Na and Al contents, which are significantly different in MSH phlogopite and tainiolite (Table 1). The Na and Al contents determined by LA–ICP–MS analyses of phlogopite are in agreement with the results of the electron-microprobe analyses on phlogopite, which were collected with a considerably smaller spot-size.

It was not possible to resolve differences between host and guest sheet-silicate by X-ray single-crystal diffraction techniques for two reasons: (1) both micas consists of the $1M$ polytype (space group $C2/m$) with parallel crystallographic axes, (2) the cell dimensions of host and guest are very similar. In some cases, fan-like spreading (<3°) of reflections around a major diffraction-maximum was observed. These can arbitrarily be interpreted as a consequence of slightly bent fibers following approximately the same crystallographic orientation as the central part of the host. In Table 2, we summarize the refined unit-cell dimensions, which are considered representative of the host (phlogopite) and overgrowth (tainiolite). The phlogopite crystals do not reveal indications of stacking faults, such as diffuse smearing, or additional weak reflections that could not be indexed with a $C2/m$ unit cell characteristic of the $1M$ polytype.

An elongate tetragonal prismatic mineral terminated by a tetragonal pyramid occurs intermingled with tainiolite fibers (Figs. 1c, d). EDS analyses (SEM) suggest that this mineral is mesolite with Na:Ca close to 1. Another aluminosilicate with a rhombohedral morphology displays a K:Ca values close to 1 (with Na ca. 10% of K) and could not be identified (Fig. 1c). Very small euhedral crystals of pyrite are ubiquitous in the sample (white phases in Fig. 1).

DISCUSSION

Crystal-chemical aspects

Our analytical results on phlogopite from MSH are unusual owing to their low level of ^{IV}Al (Table 1). In fact, excluding trioctahedral micas with tetrahedral Fe^{3+}, such as tetra-ferriphlogopite, the observed ^{IV}Al content is lower than that in all samples of natural phlogopite for which structural data are available (Brigatti & Guggenheim 2002). However, crystal structures of synthetic phlogopite-related crystals with compositions of KMg$_{2.5}$Si$_4$O$_{10}$F$_2$ (Toraya et al. 1976), KMg$_{2.75}$[Si$_{3.5}$Al$_{0.5}$]O$_{10}$F$_2$ (Toraya et al. 1978), and KMg$_3$[Si$_3$Al]O$_{10}$F$_2$ (Takeda & Morosin 1975) have been determined. In the first two compounds, the deficit in ^{IV}Al is charge-balanced by vacancies at the octahedral site.

The misfit between the sheets of tetrahedra and octahedra in mica causes deformation of the sheet of tetrahedra, lowering the sheet symmetry from hexagonal to trigonal. The degree of deformation is expressed in terms of the rotation angle α of the SiO$_4$ tetrahedra (e.g., Bailey 1984). Increasing α leads to a reduction of the lateral dimension of the sheet of terahedra. The structural studies on synthetic "fluoro-phlogopite" cited above have shown that increasing content of ^{IV}Al (from 0 to 1 apfu), which actually expands the lateral size of the sheet of tetrahedra, is partly balanced by an increase of α from 1.42° to 6.5°. In contrast to
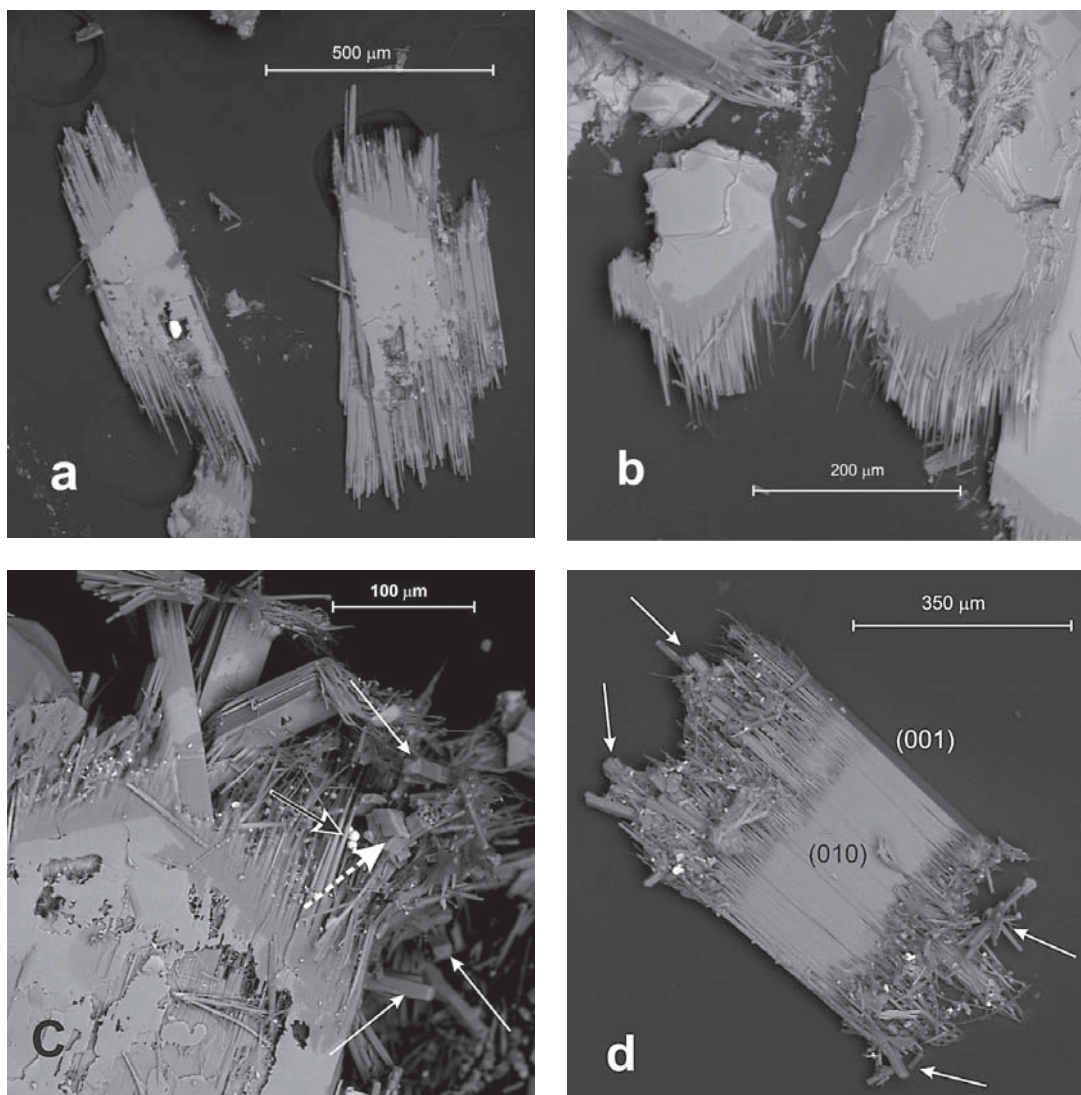
FIG. 1.   SEM images, using back-scattered electrons, of epitactic tainiolite (dark gray) on phlogopite (light gray). (a) On the right, two (001) plates of phlogopite are superimposed and slightly rotated one with respect to the other. (b) Note the unoriented fibers of tainiolite replacing dissolved phlogopite in the center of the right crystal. c) Dissolution pits in the phlogopite core. Solid white arrows mark a prismatic mineral terminated by a tetragonal pyramid for which EDS data suggest the zeolite mesolite. The dashed white arrow points to intergrown rhombs of another probable zeolite with K:Ca close to 1. The black arrow points to small crystals of pyrite (white). (d) Tainiolite block originally attached to the (010) growth front of phlogopite. Tainiolite fibers are intermingled with aggregates of mesolite, emphasized by the solid white arrows.

the synthetic samples, the MSH phlogopite acting as host for tainiolite crystallization is a stoichiometric trioctahedral mica with all octahedral sites close to fully occupied (Table 1). The low ^{IV}Al level is caused by ^{VI}Li$^+$ content requiring a higher charge in the sheet of tetrahedra. The Fe/(Fe+Mg) ratio in our material is between 0.32 and 0.25, leading to a significant exten-sion of the sheet of octahedra, compared to the synthetic samples, as indicated by increased unit-cell dimensions in the (001) plane (Table 2). The combination of high level of ^{VI}Fe^{2+} substitution and low ^{IV}Al suggests low α rotation angles for the phlogopite found as host crystals of the epitactic tainiolite.

TABLE 1. ANALYTICAL RESULTS FOR TRIOCTAHEDRAL MICAS FROM
MONT SAINT-HILAIRE AND FOR SHIROKSHINITE FROM THE KHIBINY MASSIF,
KOLA PENINSULA, RUSSIA

	Phl MSH 1	Phl1 MSH n = 9	Phl2 MSH n = 3	Tai1 MSH n = 10	Tai MSH 1[a]	Tai MSH 2[b]	Tai ideal	Shk ideal	Shk Khib. 3
SiO_2 wt.%	41.26	41.61	44.04	57.16	57.20	59.35	59.34	57.08	57.64
TiO_2	0.14	0.39	0.48	0.02	0.30	0.17	-	-	0.16
Al_2O_3	10.44	9.55	8.62	0.11	4.30	0.09	-	-	0.24
Cr_2O_3	-	-	-	0.01	-	-	-	-	-
FeO	13.46	14.45	10.56	0.22	-	0.37	-	-	1.54
MnO	0.32	0.61	0.43	-	-	0.09	-	-	0.23
MgO	18.21	15.78	17.62	19.27	17.00	19.43	19.91	19.14	19.17
CaO	-	0.06	-	-	0.19	-	-	-	-
Li_2O	n.a.	0.64	0.64	2.11	2.20	(3.90)[4]	3.69		0.00
Na_2O	0.20	0.12	0.10	2.83	0.67	0.13		7.36	7.01
K_2O	9.64	9.99	10.60	11.35	9.50	10.99	11.63	11.19	10.18
H_2O	2.44	(2.68)[4]	(2.28)[4]	(0.42)[4]	(4.34)[4]	(1.07)[4]	-	-	0.00
F	3.27	2.59	3.60	8.11	n.a.	7.18	9.38	9.03	9.19
Cl	0.04	-	-	0.10	-	-	-	-	-
F,Cl=O	-1.39	-1.09	-1.52	-3.44	n.a.	-3.02	-3.95	-3.80	-3.87
Sum	98.03	97.38	97.45	98.25	95.70	99.75	100.00	100.00	101.49
Si *apfu*	3.105	3.164	3.281	3.988	3.954	3.995	4.00	4.00	3.98
Al	0.895	0.836	0.719	0.009	0.046	0.005			0.02
Sum	4	4	4	3.996	4	4	4	4	4
Al	0.030	0.020	0.038		0.305	0.001			
Cr				0.001					
Ti	0.007	0.022	0.027	0.001	0.015	0.009			0.01
Fe	0.847	0.919	0.658	0.013		0.021			0.09
Mn	0.021	0.039	0.027			0.005			0.01
Mg	2.042	1.789	1.957	2.002	1.752	1.959	2.00	2.00	1.97
Li		0.196	0.192	0.592	0.615	1.055	1.00		
Na				0.383	0.090			1.00	0.92
Sum	2.947	2.985	2.899	2.992	2.777	3.050	3	3	3
Ca		0.005			0.014				
Na	0.029	0.018	0.014			0.017			0.02
K	0.926	0.969	1.007	1.010	0.838	0.944	1.00	1.00	0.90
Sum	0.955	0.992	1.021	1.010		0.961	1	1	0.92
OH	1.217	1.377	1.144	0.198	2	0.481			
F	0.778	0.623	0.856	1.790		1.529	2	2	2
Cl	0.005			0.012					

Phlogopite compositions are normalized on 11 atoms of oxygen per formula unit (*apfu*). [1] Lalonde *et al.* (1996), [2] Mandarino & Anderson (1989), [a] wet-chemical analysis, [b] electron-microprobe analysis, [3] Pekov *et al.* (2003), [4] values calculated; n.a.: not analyzed. Symbols: Phl: phlogopite, Shk: shirokshinite, Tai: tainiolite.

Preliminary results of the energy-dispersion analyses of tainiolite epitactic on phlogopite from MSH indicate the presence of significant Na. An external source of Na [*e.g.*, Na migration under the electron beam (Spray & Rae 1995)] must be excluded because all analyses were performed on isolated flakes of mica, as displayed in Figure 1. Furthermore, Na contents between 2.5 and 3.5 wt.% Na_2O were subsequently confirmed by EMP and LA–ICP–MS analyses. Normalization of the tainiolite data on 22 negative charges (11 O) yields the composition $(Mg_{2.00}Fe_{0.01}Li_{0.59}Na_{0.38})_{\Sigma 2.98}$ for the sheet of octahedra (Table 1). Thus the epitactic

tainiolite would represent a solid solution between tainiolite, $K(LiMg_2)Si_4O_{10}F_2$ (Toraya *et al.* 1977) and shirokshinite, $K(NaMg_2)Si_4O_{10}F_2$ (Pekov *et al.* 2003). Both structures show very similar cell dimensions and distortions (Table 2). In particular, both minerals have the sheet of tetrahedra fully expanded, giving rise to very low rotation angles (α), as already predicted for the phlogopite host. In shirokshinite, Na–Mg order is close to complete (Pekov *et al.* 2003), and Na is concentrated at the larger $M1$ site (on the mirror plane). In contrast, Li–Mg order in tainiolite is less pronounced, and Mg occupies 71% of $M1$ and 66% of $M2$ (Toraya *et al.* 1977).

The issue of ^{VI}Na in lithian micas was addressed and critically reviewed by Pekov *et al.* (2003). Their electron-microprobe results on alleged lithian micas with ^{VI}Na did not confirm the results of previous wet-chemical analyses on corresponding samples. The authors concluded that evidence of ^{VI}Na in mica obtained from wet-chemical analyses must be considered with great caution because of the possibility of contamination with impurities in the large sample required. In fact, some of the quoted results of wet-chemical analyses match stoichiometry of a mica very poorly. In all re-analyzed samples (Pekov *et al.* 2003) and also in other samples of tainiolite and polylithionite from the Khibiny massif, the Na content is less than 1 wt.% Na_2O, and (K + Na) never is over 1.0 *apfu* within standard deviations.

On the basis of the critical evaluation of older analytical results by Pekov *et al.* (2003), the epitactic tainiolite on phlogopite from MSH would seem to represent the first example of an extended solid-solution member between tainiolite and shirokshinite determined by EMP and LA–ICP–MS techniques. Thus, the conditions of formation of this unique sodian tainiolite are of special importance.

The paragenesis (Fig. 2), based on overgrowth relationships, is pectolite, $NaCa_2Si_3O_8(OH)$, followed by albite and dolomite. Phlogopite formed next, and was overgrown and partially replaced by tainiolite. Quartz then crystallized, covering most exposed surfaces. Calcite then crystallized epitactically on exposed dolomite. Mesolite was the final phase to form, and occurs as isolated crystals and clusters of crystals on quartz, phlogopite, tainiolite and dolomite. The other minor phases are post-tainiolite, but their exact location in the paragenesis cannot be established with the materials available. During this paragenesis, pectolite was partially corroded and may have served as source of Na for sodian tainiolite.

Other hand specimens from the Poudrette quarry have been reported to exhibit bladed crystals of tainiolite, close to end-member composition, without ^{VI}Na (Mandarino & Anderson 1989). For those crystals, no evidence of epitactic growth has been reported. We may speculate that the unusual sodian composition of tainiolite reported in this paper was possible because epitactic crystallization did not require a nucleation step.

Orientation of the tainiolite fibers

At first glance, it is most puzzling that the epitactic tainiolite fiber-orientation does not follow the pseudohexagonal symmetry of the sheet of tetrahedra in micas, but instead the fibers grow only parallel to [100] of phlogopite (Figs. 1a–c). Fibrous growth of sheet silicates is not common except for chrysotile and related minerals, where the sheets are rolled up to cylinders, forming hollow fibers. Such a case is completely different from fibrous tainiolite, for which a single fiber may be envisioned as a flat ribbon-like portion of a sheet silicate structure. For this reason, tainiolite fibers are very flexible and easily bent, in contrast to chrysotile fibers, which are elastic. In this context, we like to recall the Greek origin of the name tainiolite, which was derived from "tainia", a band or ribbon, which emphasizes the general tendency to form rather elongate bands or ribbons rather than the pseudohexagonal platelets typical of most other micas. Nevertheless, the fibrous habit of tainiolite observed on the MSH samples is highly unusual.

Güven (2001) described authigenic fibers of illite grown epitactically on kaolinite and mica cores found in sandstones. He observed three epitactic relationships: (1) a single set of illite laths oriented parallel to [100] of a euhedral core of kaolinite, (2) double sets of laths oriented at an angle of 120° to each other, (3) triple sets of laths following the pseudohexagonal symmetry of the
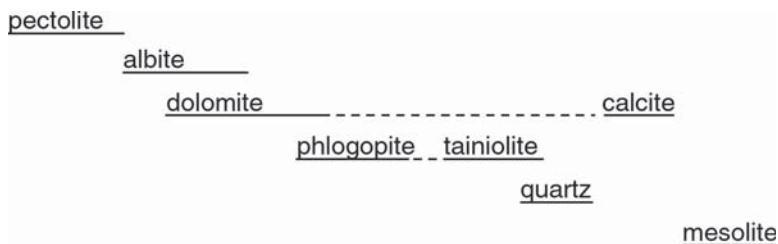

Fig. 2.   Paragenesis (early: left, late: right) of the minerals associated with the phlogopite with tainiolite overgrown.

sheet of tetrahedra. Relationship (1) is an analogue to our finding. Güven (2001) also reviewed experimental studies producing fibrous illite. In particular, diagenetic conditions (low temperature) and the presence of organic acids seem to stimulate illite-fiber precipitation. It is assumed that illite laths are metastable forms that eventually recrystallize to platy equilibrium forms.

We cannot provide direct evidence for the conditions of epitactic growth of fibrous tainiolite on phlogopite, but the mechanisms seems to be in line with the arguments stated by Güven (2001). The crystal structure of a mica provides three dominant directions of growth (Fig. 3), namely [100], [$\bar{1}$10] and [$\bar{1}\bar{1}$0]. Growth of mica parallel to [001] requires two-dimensional nucleation or screw dislocations. In contrast, tetrahedra and octahedra can be readily attached along [100], [$\bar{1}$10] and [$\bar{1}\bar{1}$0] without need of nucleation. The growth fronts (010), (110) and (1$\bar{1}$0) are parallel to the growth chains [100],

[$\bar{1}$10] and [$\bar{1}\bar{1}$0], respectively. Laths and fibers develop if the growth rate on the (010) front is slower than on the (110) and ($\bar{1}$10) fronts. Development of epitactic fibers of tainiolite along [100] and parallel to [100] of phlogopite requires special conditions. Thus, there must be some mechanism retarding growth parallel to the (010) front. The atomic configurations exposed on the (010), (110) and ($\bar{1}$10) fronts are considerably different (Fig. 3). The surface of (010) exposes terminal OH groups or F as ligands of octahedra and also densely packed rows of interlayer K (Fig. 3). This growth front must be somehow "poisoned" to explain fibrous growth parallel to [100].

Güven (2001) argued that exposed OH-groups may form complexes with organic acids by stripping off the proton, thus stopping the (010) growth front. At this point, our interpretation deviates from the one suggested by Güven (2001). Because tainiolite growth occurred
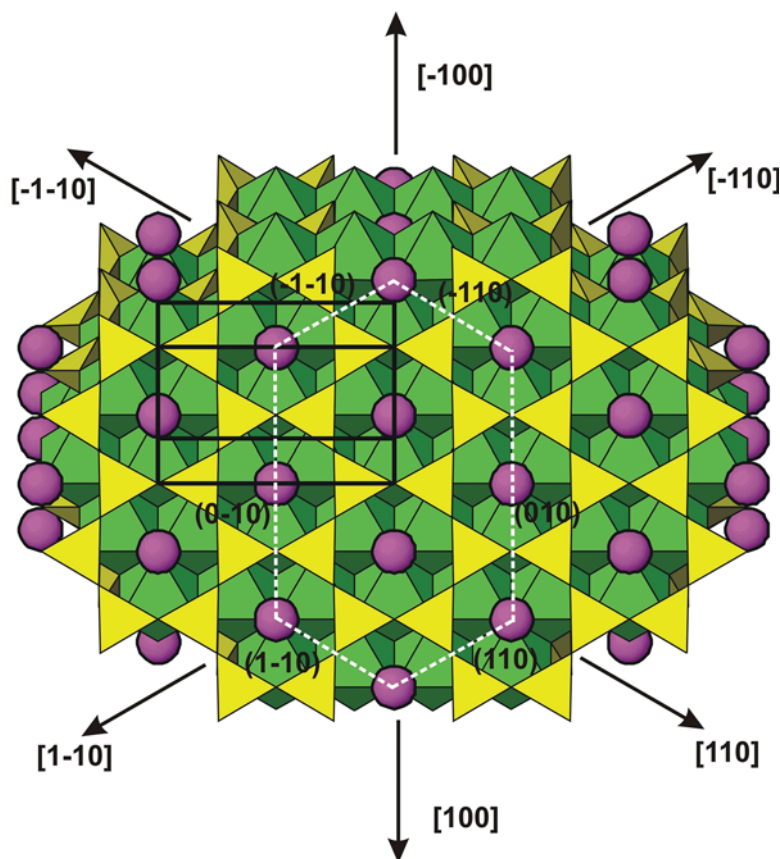

FIG. 3. Polyhedral representation of a trioctahedral mica structure, 1M polytype (space group C2/m), projected perpendicular to (001). Growth fronts (traces of crystal faces) are indicated by dashed white lines, unit-cell outlines are shown by solid black lines. Magenta spheres represent interlayer K, decorating the (010) growth surface. In tainiolite, growth of this surface is retarded due to "poisoning".

TABLE 2. CELL DIMENSIONS AND TETRAHEDRON-ROTATION ANGLE (α)
IN SOME TRIOCTAHEDRAL $C2/m$ $1M$ MICA POLYTYPES

sample	a (Å)	b (Å)	c (Å)	β (°)	V (Å^3)	α (°)	Ref.
$KMg_{2.5}Si_4O_{10}F_2$	5.253(1)	9.086(2)	10.159(1)	99.89(3)	477.7(3)	1.42	1
$KMg_{2.75}Si_{3.5}Al_{0.5}O_{10}F_2$	5.292(1)	9.164(5)	10.143(1)	100.07(2)	484.3(3)	3.63	2
$KMg_3Si_3AlO_{10}F_2$	5.3074(6)	9.195(2)	10.134(1)	100.08(1)	487.0(2)	6.50	3
$K(NaMg_2)Si_4O_{10}F_2$	5.269(2)	9.092(9)	10.198(3)	100.12(7)	481.0(1)	1.26	4
$K(LiMg_2)Si_4O_{10}F_2$	5.231(1)	9.065(2)	10.140(1)	99.86(2)	473.8(1)	1.08	5
MSH phlogopite a	5.325(2)	9.203(5)	10.233(3)	100.08(6)	493.7(4)		6
MSH phlogopite b	5.311(4)	9.204(6)	10.217(4)	99.96(6)	491.8(5)		6

References: 1 Toraya *et al.* (1976), 2 Toraya *et al.* (1978), 3 Takeda & Morosin (1975), 4 Toraya *et al.* (1977), 5 Pekov *et al.* (2003), 6 this study. For chemical variation of the phlogopite at Mont Saint-Hilaire, consult Table 1.

under hydrothermal rather than diagenetic conditions, the influence of organic acids is certainly reduced, although preserved fossils have been found in MSH marble xenoliths. However, most importantly tainiolite is a fluoro-silicate, which exposes F rather than reactive OH groups on its (010) surface. We believe that the densely packed rows of interlayer K (Fig. 3) provide the key for (010) surface "poisoning". Our hypothesis is that the invading F-, Na-, and Li-rich fluids responsible for the formation of epitactic tainiolite on phlogopite contained or liberated other inorganic polyanions (*e.g.*, CO_3^{2-}) that attached to the cationic surface and retarded (010) growth. This mechanism would explain both observations: (1) fibrous growth of tainiolite parallel to [100], and epitactic growth only parallel to [100] of phlogopite but not parallel to [1̄10] and [11̄0]. Güven (2001) interpreted the simultaneous occurrence of double and triple sets of illite fibers separated by 60° on a kaolinite core as a consequence of stacking faults in the kaolinite. The prevalence of the tainiolite fibers parallel to [100] of phlogopite is in accordance with the lack of evidence for twinning or stacking faults in phlogopite analyzed by us.

References

Armstrong, J. T. (1995): CITZAF: a package of correction programs for the quantitative electron microbeam X-ray analysis of thick polished materials, thin films, and particles. *Microbeam Anal*. **4**, 177-200.

Bailey, S.W. (1984): Crystal chemistry of true micas. *In* Micas (S.W. Bailey, ed.). *Rev. Mineral*. **13**, 13-60.

Brigatti, M.F. & Guggenheim, S. (2002): Mica crystal chemistry and the influence of pressure, temperature, and solid solution on atomistic models. *In* Micas: Crystal Chemistry and Metamorphic Petrology (H. Mottana, F.P. Sassi, J.B. Thompson & S. Guggenheim, eds.). *Rev. Mineral. Geochem*. **46**, 1-97.

Currie, K.L. (1970): An hypothesis on the origin of alkaline rocks suggested by the tectonic setting of the Monteregian Hills. *Can. Mineral*. **10**, 411-420.

Currie, K.L. (1983): An interim report on the geology and petrology of the Mont Saint-Hilaire pluton, Quebec. *Geol. Surv. Can., Pap*. **83-1B**, 39-46.

Currie, K.L., Eby, G.N. & Gittins, J. (1986): The petrology of the Mont Saint-Hilaire complex, southern Quebec: an alkaline gabbro – peralkaline syenite association. *Lithos* **19**, 65-81.

Greenwood, R.C. & Edgar, A.D. (1984): Petrogenesis of the gabbros from Mont St. Hilaire, Quebec. *Geol. J*. **19**, 353-376.

Güven, N. (2001): Mica structure and fibrous growth of illite. *Clays Clay Minerals* **49**, 189-196.

Lalonde, A.E., Rancourt, D.G. & Chao, G.Y. (1996): Fe-bearing trioctahedral micas from Mont Saint-Hilaire, Québec, Canada. *Mineral. Mag*. **60**, 447-460.

Mandarino, J.A. & Anderson, V. (1989): *Monteregian Treasures: the Minerals of Mont Saint-Hilaire, Québec*. Cambridge University Press, Cambridge, U.K.

McDonald, A.M. & Chao, G.Y. (2004): Haineaultite, a new hydrated sodium calcium titanosilicate from Mont Saint-

Hilaire, Quebec: description, structure determination and genetic implications. *Can. Mineral*. **42**, 769-780.

Pekov, I.V., Chukanov, N.V., Ferraris, G., Ivaldi, G., Pushcharovsky, D.Y. & Zadov, A. (2003): Shirokshinite, $K(NaMg_2)Si_4O_{10}F_2$, a new mica with octahedral Na from Khibiny massif, Kola Peninsula: descriptive data and structural disorder. *Eur. J. Mineral*. **15**, 447-454.

Pettke, T., Halter, W.E., Webster, J.D., Aigner-Torres, M. & Heinrich, C.A. (2004): Accurate quantification of melt inclusion chemistry by LA–ICPMS: a comparison with EMP and SIMS and advantages and possible limitations of these methods. *Lithos* **78**, 333-361.

Spray, J.G. & Rae, D.A. (1995): Quantitative electron-microprobe analysis of alkali silicate glasses: a review and user guide. *Can. Mineral*. **33**, 323-332.

Takeda, H. & Morosin, B. (1975): Comparison of observed and predicted structural parameters of mica at high temperature. *Acta Crystallogr*. **B31**, 2444-2449.

Toraya, H., Iwai, S., Marumo, F., Daimon, M. & Kondo, R. (1976): The crystal structure of tetrasilicic potassium fluor mica, $KMg_{2.5}Si_4O_{10}F_2$. *Z. Kristallogr*. **144**, 42-52.

Toraya, H., Iwai, S., Marumo, F. & Hirao, M. (1977): The crystal structure of taeniolite, $KLiMg_2Si_4O_{10}F_2$. *Z. Kristallogr*. **146**, 73-83.

Toraya, H., Iwai, S.I., Marumo, F., Nishikawa, T. & Hirao, M. (1978): The crystal structure of synthetic mica, $KMg_{2.75}Si_{3.5}Al_{0.5}O_{10}F_2$. *Mineral. J*. **9**, 210-220.

Van Velthuisen, J. (1990): A hornfels unit in the Poudrette Quarry. *Mineral. Rec*. **21**, 360-362.